Published in final edited form as:
Arterioscler Thromb Vasc Biol. 2021 October 01; 41(10): 2598–2615. doi:10.1161/ATVBAHA.120.316389.

Hypercholesterolemia Impairs Clearance of Neutrophil Extracellular Traps and Promotes Inflammation and Atherosclerotic Plaque Progression

Umesh Kumar Dhawan[1,2], **Purbasha Bhattacharya**[2,3], **Sriram Narayanan**[2], **Vijayprakash Manickam**[2], **Ayush Aggarwal**[2,3], **Manikandan Subramanian**[1,2,*]

[1]William Harvey Research Institute, Barts and The London School of Medicine and Dentistry, Queen Mary University of London, UK

[2]CSIR-Institute of Genomics and Integrative Biology, New Delhi, India

[3]Academy of Scientific and Innovative Research, India

Abstract

Objective—Hypercholesterolemia-induced NETosis and accumulation of neutrophil extracellular traps (NETs) in the atherosclerotic lesion exacerbates inflammation and is causally implicated in plaque progression. We investigated whether hypercholesterolemia additionally impairs the clearance of NETs mediated by endonucleases such as DNase1 and DNase1L3 and its implication in advanced atherosclerotic plaque progression.

Approach and results—Using a mouse model, we demonstrate that an experimental increase in the systemic level of NETs leads to a rapid increase in serum DNase activity which is critical for the prompt clearance of NETs and achieving inflammation resolution. Importantly, hypercholesterolemic mice demonstrate an impairment in this critical NET-induced DNase response with consequent delay in the clearance of NETs and defective inflammation resolution. Administration of TUDCA, a chemical chaperone that relieves endoplasmic reticulum (ER) stress, rescued the hypercholesterolemia-induced impairment in the NET-induced DNase response suggesting a causal role for ER stress in this phenomenon. Correction of the defective DNase response with exogenous supplementation of DNase1 in *Apoe*$^{-/-}$ mice with advanced atherosclerosis resulted in a decrease in plaque NET content and significant plaque remodeling with decreased area of plaque necrosis and increased collagen content. From a translational standpoint, we demonstrate that humans with hypercholesterolemia have elevated systemic extracellular DNA levels and decreased plasma DNase activity.

Conclusions—These data suggest that hypercholesterolemia impairs the NET-induced DNase response resulting in defective clearance and accumulation of NETs in the atherosclerotic plaque.

*corresponding author, **Address for correspondence:** Manikandan Subramanian, MBBS, PhD, Senior Lecturer in Cardiovascular Inflammation, William Harvey Research Institute, Centre for Biochemical Pharmacology, Barts and The London School of Medicine, Queen Mary University of London, Charterhouse Square, London EC1M6BQ, m.subramanian@qmul.ac.uk.

Disclosure
The authors declare that they have no conflict of interest.

Europe PMC Funders Author Manuscripts

Therefore, strategies aimed at rescuing this defect could be of potential therapeutic benefit in promoting inflammation resolution and atherosclerotic plaque stabilization.

Introduction

Neutrophil extracellular traps (NETs) are a potent damage-associated molecular pattern which elicits a robust inflammatory response that is critical for host defense against pathogens[1]. However, inappropriate release and persistence of NETs has been demonstrated to be maladaptive in cancers, autoimmune disorders, and several chronic inflammatory diseases including cardiometabolic disease such as atherosclerosis[2]. Therefore, prompt clearance of NETs by exonucleases such as DNase1 and DNase1L3[3] is a critical factor to prevent host tissue damage and maintain functional homeostasis.

Interestingly, in clinical conditions associated with extensive necrosis or NETosis such as myocardial infarction and sepsis, the levels of extracellular DNA as well as plasma DNase activity are known to increase[4–7]. Importantly, patients with myocardial infarction who had a lower ratio of ds-DNA/DNase activity had significantly better survival and recovery[8] suggesting an important role for an elevated level of DNase in attenuating disease pathogenesis. However, the mechanism of increase in DNase activity and whether it is mediated in response to an increase in the level of extracellular DNA is currently unknown.

In atherosclerosis, NETotic cells and NETs accumulate in atherosclerotic lesions which are causally implicated in plaque progression[9–11]. The increase in atherosclerotic plaque NET content has been attributed to hypercholesterolemia-induced neutrophilia[12] and enhanced susceptibility of neutrophils to NETosis[13]. However, whether the persistence of NETs in the atherosclerotic lesions could arise due to impairment in DNase-mediated clearance of NETs has not been explored.

Exogenous systemic administration of DNase1 can lower inflammation and prevent pathological progression of experimental disease settings in the mouse including breast cancer, lupus, lung injury, sepsis, and atherosclerosis[14]. These data suggest that impairment in the process of clearance of extracellular DNA including NETs can exacerbate disease progression and restoration of DNA clearance could be efficiently harnessed for therapy.

In this study, we report that an experimental increase in the level of NETs leads to a concomitant increase in serum DNase activity indicating the operation of a robust NET-induced DNase response. Most importantly, using a murine model, we demonstrate that the NET-induced DNase response is impaired during hypercholesterolemia via an ER-stress mediated mechanism leading to persistent elevation of extracellular ds-DNA levels, delayed inflammation resolution, and increased local and systemic inflammation. In addition, correction of the sub-optimal NET-induced DNase response by exogenous supplementation of DNase1 in a mouse model of advanced atherosclerosis led to clearance of NETs in plaques, decreased plaque inflammation and necrosis, and enhanced atherosclerotic plaque stability. These data provide novel insights into mechanisms by which hypercholesterolemia impairs inflammation resolution and promotes atherosclerotic plaque progression via defective clearance of NETs.

Europe PMC Funders Author Manuscripts

Materials and Methods

All data presented in this study are available from the corresponding author upon reasonable request.

Animals and animal maintenance

C57BL/6J mice were bred at the animal facility of CSIR-Institute of Genomics and Integrative Biology, New Delhi. *Apoe*$^{-/-}$ mice on a C57BL/6J genetic background (The Jackson Laboratory, Stock No: 002052) was obtained from CSIR-Centre for Cellular and Molecular Biology, India, and were bred as homozygotes and maintained at the animal facility of CSIR-Institute of Genomics and Integrative Biology. To induce short-term hypercholesterolemia, 8-10 wk old male *Apoe*$^{-/-}$ mice were fed a western-type diet (D12079B, Research Diets, 40% Kcal from fat, 0.2% cholesterol) ad-libitum. To generate advanced atherosclerotic plaques, 8-10 wk old female *Apoe*$^{-/-}$ mice were fed a Western-type diet ad-libitum for 16 wks. All animal protocols used in this study were approved by the Institutional Animal Ethics Committee (IAEC) of CSIR-Institute of Genomics and Integrative Biology, New Delhi.

Isolation of NETs and systemic injection

HL-60 cells cultured in RPMI supplemented with 10% FBS were incubated with 1 μM All-trans retinoic acid (ATRA R2625-50MG, Sigma) for 4 days to induce neutrophil-like differentiation following which they were treated with 100 nM PMA for 4 h to induce NETosis[15] and release of NETs. The plate-adherent NETs were scraped and collected along with the culture supernatant. Cells and cell debris were pelleted by low-speed centrifugation at 450 $\times g$ for 10 min. The NET-rich supernatant thus obtained was further centrifuged for 10 minutes at 18,000 $\times g$ at 4 °C to pellet NETs which was then resuspended in ice-cold PBS. DNA concentration was measured in the sample obtained using spectroscopy absorbance at 260/280 nm. The isolated NETs was diluted in 1X-PBS to a final concentration of 40 μg in 300 μL and injected intravenously via the lateral tail vein of 10 wk-old C57BL/6J mice. 20 μL of blood was collected by tail bleed at periodic intervals of 1, 4, and 8 h post-injection for analysis of extracellular DNA and DNase activity. The mice were euthanized at 12 h post-injection of NETs by an overdose of thiopentone sodium followed by intracardiac puncture to isolate blood for detailed analysis of several biochemical and inflammatory parameters.

Measurement of plasma and serum extracellular ds-DNA

Extracellular ds-DNA concentration was measured using Qubit™ dsDNA HS Assay Kit (Thermofisher Cat# Q32851) according to the manufacturer's protocol using either 4 μL of human plasma or 2 μL of mouse serum sample.

Single radial enzyme diffusion (SRED) assay for quantification of total DNase activity

For measuring total DNase activity in tissues, after euthanasia, the mice were perfused with PBS via intracardiac puncture. Organs were harvested and snap-frozen in liquid nitrogen and stored at −80° C until use. Organ extracts were prepared by bead homogenization (VP 43 SOP) in Tris/HCl pH 7.8. The crude extract was centrifuged at 20,000 $\times g$ for 10 min at

4° C and the supernatant was collected followed by estimation of protein content by BCA method. SRED for measuring total DNase activity in the plasma, serum, or cell culture supernatant was conducted as described previously[3]. 55 μg/mL salmon testes DNA (Sigma-Aldrich, D-1626) was resuspended in a buffer containing Mn^{2+} (20 mM Tris-HCl pH 7.8, 10 mM $MnCl_2$, 2 mM $CaCl_2$, and 2X ethidium bromide). The DNA solution was heated at 50°C for 10 minutes and mixed with an equal volume of 2% agarose (Sigma-Aldrich). The mixture was poured onto a plastic casting tray and left at room temperature till it solidified. Wells of approximately 0.1 mm size were created using a 20 μL pipette tip. 2 μL of murine serum or 4 μL of human plasma or 5 μL of 100X concentrated cell culture supernatant, or 5 μL of tissue extract were loaded into wells and gels were incubated for 6 hours at 37°C in a humidified chamber followed by image acquisition using UV excitation in Gel Doc system (Syngene G: BOX XX6). The area of DNA degradation was analyzed on Fiji (ImageJ) and the DNase activity in the sample was calculated by interpolation from standards of known DNase activity (0 – 20 U/mL).

Denaturing polyacrylamide gel electrophoresis zymography (DPZ) for measurement of DNase1 and DNase1L3 activity

DPZ was performed as described previously with some modifications[3, 16]. Briefly, sodium dodecyl sulphate (SDS)—polyacrylamide gels were prepared with 4% (v/v) stacking gels without DNA and 10% (v/v) resolving gels containing 200 μg/mL of salmon testes DNA (Sigma-Aldrich, Germany). For the detection of DNase1, 0.5 μL of murine serum or 5 μL of cell culture supernatant was mixed with 12 μL of water and 5 μL SDS gel-loading buffer. Liver and intestine were homogenized in Tris/HCL pH 7.8 buffer followed by removal of tissue debris by centrifugation at 20,000 g for 10 minutes at 4 °C. Subsequently, RIPA buffer was added, and samples were kept on ice for 30 minutes followed by centrifugation at 20,000 g for 10 minutes at 4 °C to obtain the protein fraction. 50 μg and 350μg protein were adjusted for liver and intestine respectively in 10μl volume and mixed with 5μl SDS loading buffer. The mixture was loaded onto wells and electrophoresis was carried out at 120 V in a Tris-glycine electrophoresis buffer (25 mM Tris, 192 mM glycine, 0.1% (w/v) SDS, pH 8.7). After electrophoresis, SDS was removed by washing the gels twice for 30 min each at 50°C with 10 mM Tris-HCl pH 7.8 following which the proteins were refolded by incubating the gels overnight at 37°C in a re-folding buffer (10 mM Tris-HCl pH 7.8, 3 mM $CaCl_2$, 3 mM $MgCl_2$). Images were acquired with UV excitation in a Gel Doc system followed by image quantification using Fiji.

For the detection of DNase1L3, 2 μL of serum was mixed with 12 μL of water, 5 μL SDS gel-loading buffer and 1 μL of beta-mercaptoethanol (β-ME) which inactivates DNase1 via reduction of its disulphide bridges. The mixture was heated for 5 minutes and loaded onto the gels. Electrophoresis and subsequent washing were carried out as described for DNase1. The proteins were refolded by sequential incubation of the gel for 48 h at 37°C in refolding buffer - 1 (10 mM Tris-HCl pH 7.8 containing 1 mM β-ME) followed by a further 48 h incubation at 37°C in refolding buffer - 2 (refolding buffer 1 supplemented with 3 mM $CaCl_2$ and 3 mM $MnCl_2$). Images were acquired with UV excitation in a Gel Doc system followed by image quantification using Fiji.

Europe PMC Funders Author Manuscripts

Detection of NETs in plasma by ELISA

For the detection of NETs in plasma, 96 well ELISA plate were coated with 1:1000 dilution of a polyclonal anti-myeloperoxidase antibody (Thermofisher, Cat # PA5-16672) using a carbonate-bicarbonate buffer. After blocking with 2% BSA for 1 h at room temperature, the wells were incubated with 30 μL of serum at 4°C for 12 h. After 3 washes with PBS containing 0.1% tween 20, the DNA content in the well was quantified using Quant-iT PicoGreen ds-DNA assay kit (Invitrogen, Cat # P11496) following the manufacturer's instructions. Wells incubated with genomic DNA or *in vitro* generated NETs were used as negative and positive control respectively.

Aortic root atherosclerotic lesion analysis

Eight-to-ten-weeks-old *Apoe*$^{-/-}$ female mice were fed a western-type diet for 16 weeks. Immediately after euthanasia, the mice were perfused with 1X-PBS by cardiac puncture into the left ventricle, and aortic roots, along with heart were collected and fixed in 10% neutral buffered formalin. Later, the tissues were embedded in paraffin and 8 μm-thick sections were cut using a microtome. 50-serial sections starting from the first appearance of the aortic valve were collected for analysis of aortic root atherosclerosis. Total lesion area and necrotic area were analyzed by H&E staining of 6 sections per mouse spanning the entire aortic root. For analysis of lesional collagen, the sections were stained with Mason Trichrome stain (Sigma-Aldrich) as per manufacturer's protocol.

Immunohistochemistry

Paraffin-embedded tissue specimens were sectioned, de-paraffinized with xylene, and rehydrated in decreasing concentrations of ethanol followed by 3 washes with 1X-PBS. Antigen retrieval was performed in boiling Sodium citrate buffer (10 mM Sodium citrate, 0.05% Tween-20, pH 6.0) or using Proteinase-k (20 μg/mL). The sections were then blocked with 3% fetal bovine serum in 1X-PBS for 30 min, followed by overnight - incubation at 4°C with anti-F4/80 (1:50), anti-CitH3 (1:50), anti-Dnase1 (1:50), anti-Dnase-1L3 (1:50), anti-Sm-actin (1:50). After 3 washes with 1X-PBS, the sections were further incubated with fluorescently-labeled secondary antibodies and counterstained with DAPI. Images of the stained sections were captured using a fluorescence microscope (Nikon Eclipse, Ti) and image analysis was performed using Fiji (ImageJ).

Statistical analysis

The data are presented as Mean±SEM unless otherwise stated. The n number in *in vivo* experiments represent the number of mice used in each experiment. All data sets were analyzed for normality using Shapiro-Wilk test and for equal variance using Brown-Forsythe test. For comparison of differences between two groups, a Student's t-test (for data sets with normal distribution) or a Mann-Whitney test (for datasets without normal distribution or $n<6$) was conducted. When analyzing differences between 2 or more groups, a 1-way ANOVA with Tukey's multiple comparisons test or a 2-way ANOVA with Sidak's multiple comparison test was conducted. For non-parametric data, Kruskal-Wallis followed by Dunn's multiple comparison test was conducted. All *in vitro* experiments that were conducted with n=3 biological replicates were not subjected to statistical testing since the

small sample size precludes the analysis of normal distribution or variance. These data trends are presented as Mean±SEM. All statistical analyses were performed using Graphpad Prism Ver. 9.

Results

Serum DNase1 and DNase1L3 are regulated in response to changes in systemic NET levels

We reasoned that the basal level of DNases in serum may be sufficient under physiological conditions, but the levels may need to be regulated under conditions of inflammation that elevate circulating extracellular DNA such as that released by NETosing neutrophils. To directly test this hypothesis, we experimentally increased the circulating levels of extracellular DNA in mice via intravenous injection of neutrophil extracellular traps (NETs) which were generated from PMA-treated neutrophil-like differentiated HL-60 cells[15] (Online Figure I A and B). As expected, intravenous injection of NETs led to a rapid increase in the concentration of serum extracellular ds-DNA (Figure 1A). Importantly, there was a robust increase in the level of myeloperoxidase-DNA complex, a marker of NETs, indicating that the increase in extracellular ds-DNA level is contributed by the injected NETs (Online Figure I C). Interestingly, the concentration of extracellular ds-DNA decreased over time and returned to homeostatic levels within 12 h (Figure 1A) indicating the operation of an efficient extracellular DNA clearance mechanism. Next, we asked whether the return to homeostatic levels of extracellular DNA involved an increase in the level of serum DNases. To address this question, we conducted an *in-vitro* DNA degradation assay by incubating a defined quantity of genomic DNA with serum isolated from mice injected vehicle or NETs. Interestingly, serum from NET-injected mice degraded ~70% of the input DNA as compared with only ~20% degradation observed in vehicle-injected mice (Figure 1B). These data suggested that total DNase activity is higher in the serum of NET-injected mice. To quantify the increase in DNase activity, we conducted Single Radial Enzyme Diffusion (SRED) assay as described previously[3] where the area of DNA degradation is a measure of the absolute units of DNase activity as measured using standards of known concentration of DNase. Consistent with the *in-vitro* DNA degradation assay, we observed that NET-injected mice demonstrated a ~3-fold increase in serum total DNase activity at 12 h post-injection of NETs (Figure 1C). Next, to understand the dynamics of the increase in DNase activity in response to extracellular NETs, we conducted a SRED assay and quantified the serum total DNase activity at baseline and at 1-, 4-, 8-, and 12-h post-injection of NETs. A significant increase in serum total DNase activity was observed as early as 4 h post-injection of NETs and reaching a peak at 8 h indicating a rapid active regulation of serum DNase in response to an increase in extracellular NETs (Figure 1D). It is important to note that plasma is best suited for measurement of extracellular DNA levels since it avoids *ex-vivo* release of DNA observed during coagulation. However, we observed that DNase activity in the plasma was lower as compared with serum (Online Figure I D) precluding an accurate estimation of the total DNase activity. The lower DNase activity in the plasma could potentially be due to the presence of Ca^{2+} chelators such as EDTA which are known to inhibit DNase activity. Thus, for these and future assays in mice, we have quantified DNase activity in serum.

Europe PMC Funders Author Manuscripts

The observed increase in DNase activity in the serum could either be due to an increase in the absolute levels of DNase or due to a decrease in the levels of endogenous plasma DNase inhibitors such as heparin and plasmin[16]. To understand whether the increase in serum DNase activity is mediated by an actual increase in DNase levels, we conducted Depolymerizing Gel Zymography (DPZ) as described previously[3, 16]. In this assay, DNase in the serum is denatured and resolved on a polyacrylamide gel followed by in-gel protein refolding to recover DNase activity. This assay thereby removes the confounding effects of DNase inhibitors present in serum and measures the true serum DNase levels as a function of DNase activity. Furthermore, by using specific denaturing and renaturing conditions during DPZ, the levels of the two major serum DNases, namely, DNase1 and DNase1L3 can be independently quantified[3, 16]. DPZ demonstrated that the increase in DNase activity upon injection of NETs was contributed by an increase in the levels of both DNase1 and DNase1L3 (Figure 1E). Interestingly, this increase in systemic DNase activity is observed when mice are injected with NETs or necrotic cell DNA but not when administered apoptotic cell DNA or genomic DNA that is stripped off its proteins suggesting that the DNase response is elicited by a specific DNA-protein complex that is present on NET- and necrotic cell-derived DNA but not by naked DNA (Online Figure I E). In summary, these data demonstrate that the level of key serum DNases, DNase1 and DNase1L3, are regulated in response to an increase in the level of extracellular NETs presumably to degrade and clear extracellular DNA and restore homeostasis.

Liver and intestine mediate the systemic DNase response upon injection of NETs

Under homeostatic conditions, DNase1 is known to be secreted by several tissues[14, 17]. Although the tissue source of DNase1L3 is not clearly understood, it is presumably released by cells of the myeloid lineage[14, 18]. In this context, we asked the question, which tissues respond to the systemically injected NETs and contribute to the increase in DNase1 and DNase1L3 levels observed in our experimental set-up. To address this question, we analyzed the transcript levels of DNase1 and DNase1L3 in several tissues of mice injected NETs or vehicle. Interestingly, we observed that the mRNA level of DNase1 was increased in the liver while the level of DNase1L3 was significantly increased in the intestine of NET-injected mice (Figure 2A). Other tissues examined did not show statistically significant changes in the transcript levels of either DNase1 or DNase1L3 in the NET-injected mice. Confirming the transcript data, SRED assay demonstrated increased total DNase activity in the liver and intestine of mice injected with NETs as compared with vehicle-treated mice (Figure 2B). Additionally, DPZ demonstrated that mice injected with NETs had increased levels of DNase1 in the liver and DNase1L3 in the intestine (Figure 2C). Since liver and intestine are complex tissues comprising of multiple cell types, we next addressed the cellular source of DNase1 and DNase1L3 in these tissues. Interestingly, when human hepatocyte cell line HepG2 and intestinal epithelial cell line Caco2 were incubated with NETs, we observed a robust increase in DNase activity in the cell culture supernatant using the SRED assay (Figure 2D). Importantly, a similar DNase response was observed when HepG2 cells were incubated with NETs generated by incubation of HL60 cells with lipopolysaccharide (LPS) or ionomycin[19] suggesting that the specific chemical inducer of NET does not directly mediate the DNase response (Online Figure I F). Moreover, similar to our *in vivo* data, this increase in DNase activity upon exposure to NET was contributed

by an increase in the secretion of DNase1 in the supernatant of HepG2 cells and DNase1L3 in the supernatant of Caco2 cells (Figure 2E). These data taken together suggest that liver and intestine could be a major source of secreted DNase1 and DNase1L3 respectively upon systemic encounter of NETs.

Hypercholesterolemia leads to elevated extracellular DNA and impaired DNase response

The data presented above suggest that extracellular DNA levels are tightly regulated by changes in DNase expression to enable maintenance of homeostasis. In this context, it is interesting to note that persistence of NETs and necrotic cell DNA has been reported in atherosclerotic plaques[10–12] which raises the interesting possibility that the clearance of extracellular DNA may be impaired in atherosclerosis as well as other pathological conditions.

Since hypercholesterolemia is one of the initiator and driver of atherosclerosis[20], we tested whether hypercholesterolemia could impair systemic extracellular DNA clearance. Towards this end, we set up an animal model of normocholesterolemia (WT *C57BL/6J* mice on a standard laboratory diet), moderate hypercholesterolemia (*Apoe*$^{-/-}$ mice on a standard laboratory diet), and severe hypercholesterolemia (*Apoe*$^{-/-}$ mice on a western type diet for 3 weeks) (Figure 3A). Interestingly, we observed that under basal conditions, the level of serum extracellular DNA was significantly higher in moderate and severely hypercholesterolemic mice as compared with normocholesterolemic mice (Figure 3B). In addition, there was a significant positive correlation between plasma total cholesterol levels and plasma extracellular DNA levels in this experimental model of hypercholesterolemia (Figure 3C). Since the levels of extracellular DNA is regulated by DNase activity, we next asked if a decrease in the level of serum DNase could account for the increase in ds-DNA observed during hypercholesterolemia. Surprisingly, we observed that the basal DNase activity was higher in mice with moderate hypercholesterolemia as compared with normocholesterolemic mice while the total DNase activity of severely hypercholesterolemic mice was comparable with control mice (Figure 3D). These data in conjunction with the observation of persistently high serum extracellular DNA levels in hypercholesterolemic mice raised the possibility that the NET-induced DNase response might be sub-optimal during hypercholesterolemia. To test this hypothesis and to quantify the NET-induced DNase response, we injected

NETs systemically in these mice and measured the rate of clearance of extracellular DNA from the circulation as well as the upregulation of DNase activity in the serum. We observed that the moderately hypercholesterolemic mice demonstrated a NET-induced DNase response which was comparable to control mice (Figure 3E). However, the severely hypercholesterolemic mice demonstrated a significantly blunted NET-induced DNase response upto the 12 h period of observation and was lower by about 50% as compared with the other groups of mice (Figure 3E). Next, we conducted DPZ which demonstrated that both groups of mice released DNase1 and DNase1L3 upon exposure to NETs (Figure 3F). However, the increase in the levels of DNase1 and DNase1L3 relative to baseline was significantly lower in the severely hypercholesterolemic mice indicating an impairment in the NET-induced release of both DNase1 and DNase1L3 (Figure 3F). Since there is a

decrease in the total DNase activity in the severely hypercholesterolemic mice, we asked whether this results in impairment in the rate of clearance of injected NETs. Compared with control and moderately hypercholesterolemic mice, the severely hypercholesterolemic mice had significant delay in the clearance of NETs (Figure 3G and H). Next, we measured the resolution interval[21] which we have defined as the time taken for extracellular DNA level to reach half-maximum as an indicator of efficiency of extracellular DNA clearance and return to homeostasis. The resolution interval in the severely hypercholesterolemic mice was almost double the control mice suggesting impaired clearance of extracellular DNA and delay in restoration of homeostasis (Figure 3I).

Next, we addressed whether the hypercholesterolemia-induced decrease in DNase response and increase in extracellular DNA are observed in humans. Interestingly, we observed that individuals with hypercholesterolemia (plasma total cholesterol > 200 mg/dL) had significantly higher levels of plasma extracellular DNA as compared with normocholesterolemic individuals (Figure 4A). It is important to note that there was no significant difference in age between the two groups (32.19 ± 8.79 y in normocholesterolemic vs. 34.9 ± 9.45 y in hypercholesterolemic, $p = 0.16$) but there were more females in the normocholesterolemic as compared with the hypercholesterolemic group (36.5% vs. 17.07%, respectively). Similar to our observation in the mouse model of hypercholesterolemia, there was a significant positive correlation between the levels of plasma total cholesterol and plasma extracellular DNA in humans (Figure 4B). Most importantly, hypercholesterolemic individuals had significantly lower plasma total DNase activity as compared with normocholesterolemic individuals (Figure 4C). Also, we observed a significant negative correlation between total plasma cholesterol and plasma total DNase activity (Figure 4D). These data demonstrate that hypercholesterolemia-induced impairment of DNase activity is conserved in humans and could have pathophysiological consequences.

Atherogenic dyslipidemia-induced cellular ER stress impairs the NET-induced DNase response

Since our *in-vivo* data demonstrated that hypercholesterolemia impairs the NET-induced DNase response by hampering the release of DNase from liver and intestine, we next asked whether hepatocytes exposed to hypercholesterolemic conditions have impairment in the release of DNase upon exposure to NETs *in vitro.* To model atherogenic dyslipidemia, we treated HepG2 cells with 7-ketocholesterol (7-KC), a modified oxysterol which is known to be elevated locally and systemically during atherosclerosis[22]. Interestingly, 7-KC treated HepG2 cells secreted less DNase in the culture supernatant when exposed to NETs (Figure 5A). 7-KC treatment at the dose used in our experiment did not affect cell viability (0.46% Annexin-V + in vehicle compared to 0.49% Annexin-V + upon 7-KC treatment) excluding the possibility that the decreased NET-induced DNase secretion was mediated by an increase in cell death. Consistent with the decreased release of DNase, there was increased persistence of NETs in the supernatant of 7-KC-treated HepG2 cells as compared with the control group (Figure 5B) indicating a defect in degradative clearance of extracellular NETs.

Since 7-KC is known to induce ER stress in several cell types[23, 24], we explored whether the defective NET-induced DNase response could be mediated by an ER stress-dependent

mechanism. Consistent with this hypothesis, treatment of HepG2 cells with thapsigargin, a chemical inducer of ER stress, led to decreased secretion of DNase upon incubation with NETs (Figure 5C). Next, we confirmed that 7-KC-treated HepG2 cells had higher levels of spliced form of XBP1, ATF4, and GRP78 mRNA (Figure 5D) demonstrating activation of the ER stress response in hepatocytes under conditions of atherogenic dyslipidemia. Most importantly, relieving ER stress in 7-KC treated HepG2 cells by co-incubation with a chemical chaperone TUDCA[25] (Figure 5D) led to increased levels of DNase in the culture supernatant (Figure 5E) and restoration of NET clearance (Figure 5F). Similar results were obtained when 7-KC-treated HepG2 cells were incubated with another ER stress reliever 4-PBA[26] (Figure 5G and H), suggesting that the observed phenotype is primarily due to reversal of ER stress and unlikely to be an off-target effect of the specific reagents used. These *in vitro* data taken together suggest that ER stress may be a causal factor leading to the impairment in NET-induced DNase response during atherogenic dyslipidemia.

ER stress relief rescues the defective NET-induced DNase response in hypercholesterolemic mice

Based on the *in-vitro* data above, we tested whether relieving ER stress *in-vivo* by administration of TUDCA could rescue the defective NET-induced DNase response in hypercholesterolemic mice. Towards this end, we induced severe hypercholesterolemia in *Apoe*$^{-/-}$ mice by feeding them western-type diet for 3 weeks. During this period, one group of mice was administered TUDCA (150 mg/kg intraperitoneally, daily)[27] while the control group was administered PBS. As expected, the levels of several ER stress marker genes were significantly decreased in the liver of TUDCA-treated mice (Figure 6A). It is important to note that body weight and metabolic parameters including blood glucose, plasma cholesterol, and triglyceride were similar between TUDCA-treated mice and control mice (Online Figure II A-D). Interestingly, we observed that the basal level of extracellular ds-DNA was lower in the TUDCA-treated mice as compared with control mice (Figure 6B). Consistent with the lowering of serum extracellular ds-DNA levels, TUDCA-treated mice showed elevated basal serum DNase activity (Figure 6C). Next, we injected NETs in these mice to analyze the NET-induced DNase response and efficiency of NET clearance. We observed that the TUDCA-treated hypercholesterolemic mice showed a significantly higher total serum DNase activity as compared with control hypercholesterolemic mice upon injection of NETs (Figure 6D). DPZ revealed that this increase in plasma DNase activity was contributed by an increase in the levels of both DNase1 and DNase1L3 (Figure 6E). Additionally, liver and intestine of TUDCA-treated mice demonstrated increased total DNase activity (Figure 6F) and increased levels of DNase1 and DNase1L3 respectively (Figure 6G) suggesting restoration of NET-induced DNase activity in these tissues. Most importantly, the rate of clearance of extracellular DNA was accelerated (Figure 6H) and the resolution interval was significantly shortened (Figure 6I) in TUDCA-treated mice as compared with control mice. Consistent with the accelerated clearance of extracellular DNA, the expression of pro-inflammatory genes in the spleen (Online Figure II E) and the expression level of a pro-inflammatory cytokine IP-10 in the plasma was significantly decreased in the TUDCA-treated mice (Online Figure II F and G). These data suggest that atherogenic dyslipidemia-induced ER stress leads to defective NET-induced DNase response

with consequent impairment in the clearance of extracellular DNA and exacerbated systemic inflammation.

DNase1 treatment decreases atherosclerotic plaque extracellular DNA content, inflammation, and necrotic core formation

Previous studies have shown that accumulation of extracellular DNA, particularly NETotic, necrotic, and necroptotic DNA is involved in atherosclerotic plaque progression[10–12]. Interestingly, treatment of atherosclerosis-prone mice with DNase1 has been demonstrated to prevent plaque progression in early atherosclerosis[13, 28] and promote plaque regression in diabetic mice[29]. However, whether correction of the sub-optimal DNase response via exogenous administration of DNase1 could have beneficial effects in the context of clinically relevant advanced atherosclerosis parameters such as plaque necrosis and collagen deposition are unknown. To this end, we fed *Apoe*$^{-/-}$ mice a high fat-high cholesterol western-type diet (WD) for 16 weeks which leads to generation of advanced atherosclerotic plaques characterized by large necrotic areas. Post 16 weeks of WD feeding, the mice were randomized into two groups with one group of mice receiving DNase1 (RNase-free DNase1 from bovine pancreas, Sigma D7291, 400 U, intravenously)[28] three times a week for 4 weeks, while the other group was administered an equal volume of 1X-PBS as control. At the end of 4 weeks of treatment, both groups of mice had similar body weight and metabolic parameters including blood glucose, total cholesterol, and triglycerides (Online Figure III A-D). As expected, the plasma total DNase activity was significantly higher in mice receiving DNase1 (Figure 7A). Consistent with an increase in serum DNase activity, there was a significant decrease in the serum extracellular ds-DNA levels in mice administered DNase1 (Figure 7B) reaching levels similar to that observed in *Apoe*$^{-/-}$ mice on a standard laboratory diet. Most importantly, aortic root atherosclerotic lesional NET content, measured as the extent of lesions that stain positive with anti-citrullinated H3 antibody, was significantly lower in the DNase1-treated mice (Figure 7C and Online Figure III F). In addition, the DNase1-treated mice demonstrated a significant decrease in the plaque necrotic area (Figure 7D), an increase in lesional collagen content (Figure 7E) and smooth muscle cell numbers (Figure 7F), and a decrease in plaque macrophage content (Figure 7F). Since, the total atherosclerotic lesion area is not significantly different between the two groups of mice (Figure 7D), these data taken together suggest that DNase1 treatment leads to significant cellular and structural remodeling of atherosclerotic lesions. Importantly, DNase1 treatment led to a significant decrease in atherosclerotic plaque inflammation as demonstrated by the decreased expression of pro-inflammatory genes such as *Tnf, Ifng, Ifnb,* and *Mx1* (Figure 7G). Also, DNase1-treated mice had lower systemic inflammation as demonstrated by decreased levels of pro-inflammatory gene expression in spleen (Online Figure III E) and lower levels of several pro-inflammatory cytokines in the plasma (Figure 7H). These data suggest that therapeutic increase in DNase activity to overcome the sub-optimal NET-induced DNase response in hypercholesterolemia leads to lowering of systemic inflammation and promotes beneficial cellular remodeling of plaques in advanced atherosclerosis.

Europe PMC Funders Author Manuscripts

Macrophage-mediated clearance of NETs is mediated by secretion of DNase1 and DNase1L3

The data presented so far suggests that hypercholesterolemia impairs systemic NET-induced DNase response and delays inflammation resolution and that the correction of this response by exogenous administration of DNase1 results in clearance of NETs in atherosclerotic lesions and promotes beneficial plaque remodeling. In this context, immunofluorescence analysis of atherosclerotic lesions from 16 wk WD-fed *Apoe*$^{-/-}$ mice demonstrated that plaque macrophages stain positive for intracellular DNase1 and DNase1L3 (Figure 8A and Online Figure IV A-B). Additionally, analysis of publicly available RNA-sequencing data of atherosclerotic plaques[30] revealed that lesional macrophages express transcripts for both DNase1 and DNase1L3 (Online Figure IV C). These data taken together suggest that plaque macrophages could be a local source of DNases.

Although macrophages express transcripts for DNase1 and DNase1L3 and demonstrate intracellular protein expression, we asked whether macrophages exposed to NETs have the ability to sense NETs and respond via secretion of DNase1 or DNase1L3. Interestingly, supernatants from BMDMs incubated with NETs demonstrated a significant increase in DNase activity (Figure 8B). Indeed, a similar response was observed in human THP-1 macrophage-like cells (Online Figure IV D) and in human peripheral blood monocyte-derived macrophages (Online Figure IV E) demonstrating that both murine and human macrophages have the ability to sense NETs and respond via secretion of DNases. Additionally, we demonstrate that the increased DNase activity in the supernatant is contributed by secretion of both DNase1 and DNase1L3 (Online Figure IV F).

Next, we asked whether the secreted DNase is physiologically relevant for mediating the clearance of NETs. Indeed, almost 90% of the input NETs was cleared from the supernatant within 12 h of incubation with macrophages (Figure 8C). In addition, we observed that macrophages phagocytose fragments of NETs within 2-3 h of incubation (Online Figure IV G). Interestingly, incubation of macrophages with NETs in the presence of aprotinin and plasmin, inhibitors of DNase1 and DNase1L3 respectively[16], led to a decrease in the percent macrophages that phagocytosed NETs (Online Figure IV H) and a decrease in the clearance of NETs (Online Figure IV I). These data suggest that local secretion of DNases by macrophages could promote extracellular degradation of NETs into smaller fragments which in turn could enhance the ability of macrophages to efficiently clear NETs via phagocytosis.

Atherogenic lipids induce ER stress and impair secretion of DNase1 and DNase1L3

Since, our *in-vivo* data demonstrates that hypercholesterolemia impairs the NET-induced DNase response, we next asked whether macrophages exposed to hypercholesterolemic conditions have impairment in the release of DNase upon exposure to NETs. To model atherogenic dyslipidemia, we treated BMDMs with 7-KC which leads to formation of foamy macrophages similar to that observed in atherosclerotic plaques[31]. Interestingly, 7-KC treated macrophages secreted lower levels of DNase upon exposure to NETs as compared with control macrophages exposed to NETs (Figure 8D). This decrease in DNase activity was due to an impairment in the secretion of both DNase1 and DNase1L3 (Online Figure

V A). Consistent with a decrease in DNase secretion, 7-KC treated macrophages showed significantly decreased clearance of NETs (Figure 8E) and lower level of engulfment of NETs (Online Figure V B).

As shown above, the engulfment of NETs by macrophages is facilitated by DNase-mediated degradation of NETs into smaller fragments. Thus, we reasoned that the decreased efficiency of engulfment of NETs in 7-KC-treated macrophages could be mediated by the impairment in NET-induced DNase secretion. Consistent with this hypothesis, we observed that the efficiency of engulfment of NETs of 7-KC-treated macrophages was similar to control macrophages when the activity of DNase1 and DNase1L3 are inhibited by treatment with aprotinin and plasmin respectively (Online Figure V C). Similarly, 7-KC-treated macrophages demonstrated no defect in the engulfment of pre-digested NETs (Online Figure V D). These data together suggest that the defect in engulfment of NETs observed in 7-KC-treated macrophages was primarily due to the decrease in secretion of DNases which impairs its ability to fragment NETs into smaller “digestible” fragments.

Next, we explored whether the defective DNase secretion in 7-KC-treated macrophages is mediated by ER stress[32, 33]. Similar to our *in vivo* data, we observed that administration of TUDCA to 7-KC-treated macrophages led to ER stress relief (Online Figure V E) and reversed the impairment in NET-induced DNase secretion (Figure 8F). Consistent with an increase in secreted DNase activity, the efficiency of NET clearance and NET engulfment of TUDCA-treated 7KC-macrophages was restored to a level similar to that of control macrophages (Figure 8G and H). Similar results were obtained when 7-KC-treated macrophages were incubated with azoramide[26] (Online Figure V F), another known ER stress reliever. These data taken together suggest that ER stress may be a causal factor leading to the impairment in NET-induced DNase response both systemically and within the atherosclerotic plaque during atherogenic dyslipidemia.

Discussion

There is overwhelming evidence of the pathogenic role of excessive NETosis and persistence of extracellular DNA in promoting disease progression with consequent adverse pathological and clinical outcomes[2, 34]. Previous studies have highlighted the critical role of plasma DNases in the clearance of extracellular DNA and maintenance of tissue homeostasis[14]. Indeed, lower basal DNase activity, either due to mutations in DNase1 or DNase1L3[35, 36], or the presence of plasma DNase inhibitors[37, 38], has been implicated to adversely impact disease outcomes, particularly in autoimmune lupus, myocardial infarction, sepsis, acute pancreatitis, cancers, NAFLD, and cirrhosis[14]. In this context, our findings demonstrate how a common pathological condition such as hypercholesterolemia impairs systemic DNase activity leading to delayed clearance of NETs and enhanced inflammation with important consequence in atherosclerosis progression and possibly other chronic inflammatory diseases.

Previous studies have demonstrated a correlation between an increase in extracellular DNA levels with concomitant increase in plasma DNase activity such as in myocardial infarction, sepsis, and acute pancreatitis[6, 8]. Since, liver is one of the major source of DNase1[17], it was

not clear whether in these clinical conditions of acute inflammation, the increase in DNase activity was part of an acute phase reaction or a specific response to an increase in plasma extracellular DNA. Our study demonstrates that an increase in systemic levels of NETs can be sensed by certain tissue or cell types and set in motion a response by secreting DNases to promote degradative clearance of NETs and restoration of tissue homeostasis.

While it is evident that NETs are sensed by certain cellular receptors which then mediates the DNase secretion response, the nature and identity of this receptor(s) and the downstream signaling leading to DNase release is currently unknown. Since the increase in DNase secretion *in-vivo* and *in-vitro* is elicited only upon exposure to NETs and not by nuclear DNA stripped off its proteins, our data suggests that the DNase response is mediated by sensing the DNA-protein complex. In this context, a recent study identified CCDC25 as a plasma membrane-localized receptor on cancer cells that binds exclusively to the DNA component of NETs and mediates downstream signaling involving activation of ILK-β-parvin pathway that enhances cell motility and cancer metastasis[39]. Given that the DNase response we observe is elicited only by the DNA-protein complex and not by the naked-DNA, it is unlikely that CCDC25 is involved in this response. This raises the interesting possibility of the existence of additional NET binding receptors which might be expressed in a tissue or cell type-specific manner that elicits functionally distinct responses.

Additionally, in contrast to the current notion that myeloid cells such as macrophages and dendritic cells are the major source of DNase1L3[18], our data demonstrates that intestinal epithelial cells are also capable of producing and secreting DNase1L3 in response to an increase in the systemic levels of NETs. Supporting these data, human protein atlas demonstrates that human intestinal tissue including epithelial cells demonstrate moderate levels of DNase1L3 immunostaining. Although the levels of Dnase1L3 mRNA and DNase1L3 protein are increased in the murine intestine upon exposure to NETs, the relative contribution of intestine-secreted DNase1L3 to the overall systemic increase in DNase activity can be unraveled only by tissue-specific knockout of DNase1L3. Moreover, our study demonstrates that both murine and human macrophages exposed to extracellular NETs have the ability to secrete significant quantities of DNase1 that is functionally relevant for DNA degradation *in-vitro.* In addition to the extracellular degradation of DNA by macrophage-secreted DNase, our data also suggests an important role for the secreted DNases in facilitating macrophage-mediated engulfment via digestion of DNA into smaller fragments, which leads to enhanced intracellular phago-lysosomal degradation of DNA. These data are consistent with previous studies[40, 41] which demonstrated that EDTA, which chelates divalent cations such as Ca^{2+}, Mg^{2+}, and Mn^{2+} and blocks DNase activity, leads to decreased clearance of NETs by macrophages. Since, EDTA could have several non-specific effects including inhibitory activity on phagocytic processes, our approach of specifically inhibiting the activity of DNase1 and DNase1L3 using aprotinin and plasmin is a more definitive demonstration of the co-operative role played by macrophage-secreted DNase in phagocytic clearance of NETs. Future studies using mice with macrophage-specific knockout of DNase1 and DNase1L3 (DNase1 $^{flox/flox}$ /DNase1L3$^{flox/flox}$ mice are currently unavailable) will be required to specifically understand the role of locally produced macrophage secreted DNases in extracellular NET clearance and inflammation resolution during sterile inflammation such as in atherosclerosis.

Since persistent extracellular DNA is highly pro-inflammatory, its prompt clearance is essential for maintaining immune homeostasis. Consistent with this notion, we observe that the NET-induced DNase response is a rapid response demonstrating significant elevation in DNase levels within 4 hours of elevation of extracellular DNA. Interestingly, *in vitro,* there is a significant increase in the release of DNase as early as 1-hour post exposure to NETs raising the possibility that there may be a quick exocytotic release of DNase which are known to be stored in pre-formed granules[42]. This quick release may be followed by a transcriptional response that sustains the elevated levels of tissue and systemic DNase activity in response to increased NET levels.

A previous study[28] demonstrated that exogenous administration of DNase1 decreases atherosclerotic lesion area in *Apoe*$^{-/-}$ mice fed a high-fat diet for 6 weeks suggesting a beneficial effect of DNase1-mediated clearance of NETs in lowering inflammation and protecting against early atherosclerosis. Similarly, the administration of DNase1 improved the regression of atherosclerotic plaques in diabetic *Ldlr*$^{-/-}$ mice when switched to a standard laboratory diet[29]. Complementing the findings of these studies, our results in a mouse model of advanced atherosclerosis demonstrate that restoration of the defective sub-optimal DNase response during hypercholesterolemia by exogenous administration of DNase1 aids in the lowering of local and systemic inflammation, decreases necrotic area in the plaque, and increases lesional collagen content. Consistent with a previous report[43], we did not observe any significant change in the atherosclerotic lesion area upon administration of DNase1. It is important to note that in humans, the extent of plaque necrosis, but not the total lesion area, is correlated with “rupture-prone” vulnerable plaques[44] which are causally associated with the development of clinical outcomes including myocardial infarction and stroke. In this context, our data suggest that DNase1 administration could have beneficial effects even in established advanced atherosclerotic plaques resulting in significant atherosclerotic plaque remodeling. Since DNase1 is approved for clinical use in patients with cystic fibrosis[45], further studies to test the efficacy of DNase1 as a therapeutic target in high-risk patients with advanced atherosclerosis is warranted.

Using 7-ketocholesterol, a pathophysiologically relevant ER stressor in the context of atherogenic dyslipidemia, we have demonstrated that ER stress impairs the NET-induced DNase response and results in delayed clearance of extracellular DNA. In theory, ER stress could affect the recognition of extracellular DNA by decreasing the expression level of the putative NET receptor thereby decreasing the efficiency of DNA sensing. However, this seems unlikely, since we did not observe significant difference in the binding efficiency of NETs in ER stressed-macrophages (unpublished data). Alternately, ER stress could affect the signaling downstream of the putative NET receptor and impair trafficking of DNase-containing vesicles to the plasma membrane. Indeed, ER stress is known to impair secretory processes by inhibiting focal exocytosis in an ATF4-TRB3 dependent manner in pancreatic β-cells during diabetes[46]. Whether such a mechanism is responsible for the decreased secretion of DNases by macrophages and other cell types remains to be explored.

Interestingly, our demonstration that ER stress leads to the maladaptive DNase response raises the interesting possibility that this phenomenon may be broadly applicable to several diseases associated with chronic ER stress such as diabetes, COPD, NAFLD etc. Although

this is a speculation and needs a separate study, consistent with this concept, increased levels of plasma extracellular DNA is considered an independent risk factor and an indicator of poor prognosis in NAFLD[47] and COPD[48].

In summary, our study demonstrates the existence of a NET-induced DNase response which acts as a critical feedback mechanism to maintain systemic levels of NETs within narrow physiological limits. Further, we suggest that an impairment of this NET-induced DNase response, such as during hypercholesterolemia, impairs inflammation resolution and promotes disease progression which may result in adverse clinical outcomes. These data suggest that the accumulation of NETs in atherosclerotic plaques and systemically is mediated via a “two-hit pathway” involving hypercholesterolemia-induced enhancement of NETosis and release of NETs[12, 13] coupled to impaired DNase mediated clearance of NETs. These findings open novel therapeutic opportunities to explore strategies aimed at reversing the defective NET-induced DNase response during hypercholesterolemia in an effort to stall or reverse the progression of atherosclerosis and other chronic inflammatory diseases.

Supplementary Material

Refer to Web version on PubMed Central for supplementary material.

Acknowledgements

UD, PB, SN, and VP designed and conducted experiments and analysed the data. AA conducted analysis of publicly available microarray and RNA-sequencing data. UD and MS conceptualized the study, wrote, and edited the manuscript. We thank Dr. Shantanu Sengupta and Dr. Vivek Natarajan (CSIR-Institute of Genomics and Integrative Biology, New Delhi) for helpful discussions throughout the project.

Sources of Funding

This study was supported by research funding from the DBT-Wellcome Trust India Alliance Fellowship (Grant number IA/I/17/2/503295) to MS and Barts Charity, UK (MS). UD and PB were supported by Senior research fellowship from the Department of Biotechnology, India, and the Council of Scientific and Industrial Research, India, respectively.

Nonstandard Abbreviations and Acronyms

NETs	Neutrophil extracellular traps
ER	Endoplasmic reticulum
ds-DNA	Double standard DNA
DPZ	Denaturing polyacrylamide gel electrophoresis zymography
SRED	Single radial enzyme diffusion
7-KC	7-ketocholesterol
BMDMs	Bone-Marrow Derived Macrophage

References

1. Kaplan MJ, Radic M. Neutrophil extracellular traps: Double-edged swords of innate immunity. J Immunol. 2012; 189 :2689–2695. [PubMed: 22956760]
2. Jorch SK, Kubes P. An emerging role for neutrophil extracellular traps in noninfectious disease. Nat Med. 2017; 23 :279–287. [PubMed: 28267716]
3. Jiménez-Alcázar M, Rangaswamy C, Panda R, Bitterling J, Simsek YJ, Long AT, Bilyy R, Krenn V, Renné C, Renné T, Kluge S, et al. Host dnases prevent vascular occlusion by neutrophil extracellular traps. Science. 2017; 358 1202 [PubMed: 29191910]
4. Antonatos D, Patsilinakos S, Spanodimos S, Korkonikitas P, Tsigas D. Cell-free DNA levels as a prognostic marker in acute myocardial infarction. Ann N Y Acad Sci. 2006; 1075 :278–281. [PubMed: 17108221]
5. Liu J, Yang D, Wang X, Zhu Z, Wang T, Ma A, Liu P. Neutrophil extracellular traps and dsdna predict outcomes among patients with st-elevation myocardial infarction. Scientific Reports. 2019; 9 11599 [PubMed: 31406121]
6. Meng W, Paunel-Görgülü A, Flohé S, Witte I, Schädel-Höpfner M, Windolf J, Lögters TT. Deoxyribonuclease is a potential counter regulator of aberrant neutrophil extracellular traps formation after major trauma. Mediators Inflamm. 2012; 2012 149560-149560 [PubMed: 22315507]
7. Kawai Y, Yoshida M, Arakawa K, Kumamoto T, Morikawa N, Masamura K, Tada H, Ito S, Hoshizaki H, Oshima S, Taniguchi K, et al. Diagnostic use of serum deoxyribonuclease i activity as a novel early-phase marker in acute myocardial infarction. Circulation. 2004; 109 :2398–2400. [PubMed: 15148274]
8. Ondracek AS, Hofbauer TM, Wurm R, Arfsten H, Seidl V, Früh A, Seidel S, Hubner P, Mangold A, Goliasch G, Heinz G, et al. Imbalance between plasma double-stranded DNA and deoxyribonuclease activity predicts mortality after out-of-hospital cardiac arrest. Resuscitation. 2020; 151 :26–32. [PubMed: 32251701]
9. Megens RT, Vijayan S, Lievens D, Döring Y, van Zandvoort MA, Grommes J, Weber C, Soehnlein O. Presence of luminal neutrophil extracellular traps in atherosclerosis. Thromb Haemost. 2012; 107 :597–598. [PubMed: 22318427]
10. Franck G, Mawson TL, Folco EJ, Molinaro R, Ruvkun V, Engelbertsen D, Liu X, Tesmenitsky Y, Shvartz E, Sukhova GK, Michel JB, et al. Roles of pad4 and netosis in experimental atherosclerosis and arterial injury: Implications for superficial erosion. Circ Res. 2018; 123 :33–42. [PubMed: 29572206]
11. Döring Y, Libby P, Soehnlein O. Neutrophil extracellular traps participate in cardiovascular diseases. Circulation Research. 2020; 126 :1228–1241. [PubMed: 32324499]
12. Drechsler M, Megens RTA, Zandvoort Mv, Weber C, Soehnlein O. Hyperlipidemia-triggered neutrophilia promotes early atherosclerosis. Circulation. 2010; 122 :1837–1845. [PubMed: 20956207]
13. Warnatsch A, Ioannou M, Wang Q, Papayannopoulos V. Neutrophil extracellular traps license macrophages for cytokine production in atherosclerosis. Science. 2015; 349 :316. [PubMed: 26185250]
14. Keyel PA. Dnases in health and disease. Developmental Biology. 2017; 429 :1–11. [PubMed: 28666955]
15. Remijsen Q, Kuijpers TW, Wirawan E, Lippens S, Vandenabeele P, Vanden Berghe T. Dying for a cause: Netosis, mechanisms behind an antimicrobial cell death modality. Cell Death Differ. 2011; 18 :581–588. [PubMed: 21293492]
16. Napirei M, Ludwig S, Mezrhab J, Klöckl T, Mannherz HG. Murine serum nucleases - contrasting effects of plasmin and heparin on the activities of dnase1 and dnase1-like 3 (dnase1l3). The FEBS Journal. 2009; 276 :1059–1073. [PubMed: 19154352]
17. Ludwig S, Mannherz HG, Schmitt S, Schäffer M, Zentgraf H, Napirei M. Murine serum deoxyribonuclease 1 (dnase1) activity partly originates from the liver. The International Journal of Biochemistry & Cell Biology. 2009; 41 :1079–1093. [PubMed: 18973821]

18. Sisirak V, Sally B, D'Agati V, Martinez-Ortiz W, Özçakar ZB, David J, Rashidfarrokhi A, Yeste A, Panea C, Chida AS, Bogunovic M, et al. Digestion of chromatin in apoptotic cell microparticles prevents autoimmunity. Cell. 2016; 166 :88–101. [PubMed: 27293190]
19. Thiam HR, Wong SL, Qiu R, Kittisopikul M, Vahabikashi A, Goldman AE, Goldman RD, Wagner DD, Waterman CM. Netosis proceeds by cytoskeleton and endomembrane disassembly and pad4-mediated chromatin decondensation and nuclear envelope rupture. Proc Natl Acad Sci U S A. 2020; 117 :7326–7337. [PubMed: 32170015]
20. Williams KJ, Tabas I. The response-to-retention hypothesis of early atherogenesis. Arterioscler Thromb Vasc Biol. 1995; 15 :551–561. [PubMed: 7749869]
21. Bannenberg GL, Chiang N, Ariel A, Arita M, Tjonahen E, Gotlinger KH, Hong S, Serhan CN. Molecular circuits of resolution: Formation and actions of resolvins and protectins. J Immunol. 2005; 174 :4345–4355. [PubMed: 15778399]
22. Brown AJ, Jessup W. Oxysterols and atherosclerosis. Atherosclerosis. 1999; 142 :1–28. [PubMed: 9920502]
23. Tabas I. The role of endoplasmic reticulum stress in the progression of atherosclerosis. Circulation research. 2010; 107 :839–850. [PubMed: 20884885]
24. Myoishi M, Hao H, Minamino T, Watanabe K, Nishihira K, Hatakeyama K, Asada Y, Okada K-i, Ishibashi-Ueda H, Gabbiani G, Bochaton-Piallat M-L, et al. Increased endoplasmic reticulum stress in atherosclerotic plaques associated with acute coronary syndrome. Circulation. 2007; 116 :1226–1233. [PubMed: 17709641]
25. Ozcan U, Yilmaz E, Ozcan L, Furuhashi M, Vaillancourt E, Smith RO, Görgün CZ, Hotamisligil GS. Chemical chaperones reduce er stress and restore glucose homeostasis in a mouse model of type 2 diabetes. Science. 2006; 313 :1137–1140. [PubMed: 16931765]
26. Fu S, Yalcin A, Lee GY, Li P, Fan J, Arruda AP, Pers BM, Yilmaz M, Eguchi K, Hotamisligil GS. Phenotypic assays identify azoramide as a small-molecule modulator of the unfolded protein response with antidiabetic activity. Science Translational Medicine. 2015; 7 292ra298
27. Amin A, Choi SK, Galan M, Kassan M, Partyka M, Kadowitz P, Henrion D, Trebak M, Belmadani S, Matrougui K. Chronic inhibition of endoplasmic reticulum stress and inflammation prevents ischaemia-induced vascular pathology in type ii diabetic mice. J Pathol. 2012; 227 :165–174. [PubMed: 22081301]
28. Liu Y, Carmona-Rivera C, Moore E, Seto NL, Knight JS, Pryor M, Yang Z-H, Hemmers S, Remaley AT, Mowen KA, Kaplan MJ. Myeloid-specific deletion of peptidylarginine deiminase 4 mitigates atherosclerosis. Frontiers in Immunology. 2018; 9
29. Josefs T, Barrett TJ, Brown EJ, Quezada A, Wu X, Voisin M, Amengual J, Fisher EA. Neutrophil extracellular traps promote macrophage inflammation and impair atherosclerosis resolution in diabetic mice. JCI Insight. 2020; 5
30. Goo YH, Son SH, Yechoor VK, Paul A. Transcriptional profiling of foam cells reveals induction of guanylate-binding proteins following western diet acceleration of atherosclerosis in the absence of global changes in inflammation. J Am Heart Assoc. 2016; 5 e002663 [PubMed: 27091181]
31. Hayden JM, Brachova L, Higgins K, Obermiller L, Sevanian A, Khandrika S, Reaven PD. Induction of monocyte differentiation and foam cell formation in vitro by 7-ketocholesterol. J Lipid Res. 2002; 43 :26–35. [PubMed: 11792719]
32. Myoishi M, Hao H, Minamino T, Watanabe K, Nishihira K, Hatakeyama K, Asada Y, Okada K, Ishibashi-Ueda H, Gabbiani G, Bochaton-Piallat ML, et al. Increased endoplasmic reticulum stress in atherosclerotic plaques associated with acute coronary syndrome. Circulation. 2007; 116 :1226–1233. [PubMed: 17709641]
33. Tabas I, Kitakaze M. The role of endoplasmic reticulum stress in the progression of atherosclerosis. Circulation Research. 2010; 107 :839–850. [PubMed: 20884885]
34. Papayannopoulos V. Neutrophil extracellular traps in immunity and disease. Nature Reviews Immunology. 2018; 18 :134–147.
35. Yasutomo K, Horiuchi T, Kagami S, Tsukamoto H, Hashimura C, Urushihara M, Kuroda Y. Mutation of dnase1 in people with systemic lupus erythematosus. Nat Genet. 2001; 28 :313–314. [PubMed: 11479590]

36. Al-Mayouf SM, Sunker A, Abdwani R, Abrawi SA, Almurshedi F, Alhashmi N, Al Sonbul A, Sewairi W, Qari A, Abdallah E, Al-Owain M, et al. Loss-of-function variant in dnase1l3 causes a familial form of systemic lupus erythematosus. Nature Genetics. 2011; 43 :1186–1188. [PubMed: 22019780]
37. Sallai K, Nagy E, Derfalvy B, Müzes G, Gergely P. Antinucleosome antibodies and decreased deoxyribonuclease activity in sera of patients with systemic lupus erythematosus. Clinical and Diagnostic Laboratory Immunology. 2005; 12 :56–59. [PubMed: 15642985]
38. Lazarides E, Lindberg U. Actin is the naturally occurring inhibitor of deoxyribonuclease i. Proc Natl Acad Sci U S A. 1974; 71 :4742–4746. [PubMed: 4140510]
39. Yang L, Liu Q, Zhang X, Liu X, Zhou B, Chen J, Huang D, Li J, Li H, Chen F, Liu J, et al. DNA of neutrophil extracellular traps promotes cancer metastasis via ccdc25. Nature. 2020; 583 :133–138. [PubMed: 32528174]
40. Farrera C, Fadeel B. Macrophage clearance of neutrophil extracellular traps is a silent process. J Immunol. 2013; 191 :2647–2656. [PubMed: 23904163]
41. Haider P, Kral-Pointner JB, Mayer J, Richter M, Kaun C, Brostjan C, Eilenberg W, Fischer MB, Speidl WS, Hengstenberg C, Huber K, et al. Neutrophil extracellular trap degradation by differently polarized macrophage subsets. Arteriosclerosis, Thrombosis, and Vascular Biology. 2020; 40 :2265–2278.
42. Napirei M, Wulf S, Eulitz D, Mannherz HG, Kloeckl T. Comparative characterization of rat deoxyribonuclease 1 (dnase1) and murine deoxyribonuclease 1-like 3 (dnase1l3). Biochem J. 2005; 389 :355–364. [PubMed: 15796714]
43. Soehnlein O, Ortega-Gómez A, Döring Y, Weber C. Neutrophil-macrophage interplay in atherosclerosis: Protease-mediated cytokine processing versus net release. Thromb Haemost. 2015; 114 :866–867. [PubMed: 26310276]
44. Finn AV, Nakano M, Narula J, Kolodgie FD, Virmani R. Concept of vulnerable/unstable plaque. Arteriosclerosis, Thrombosis, and Vascular Biology. 2010; 30 :1282–1292.
45. Fuchs HJ, Borowitz DS, Christiansen DH, Morris EM, Nash ML, Ramsey BW, Rosenstein BJ, Smith AL, Wohl ME, The pulmozyme study group. Effect of aerosolized recombinant human dnase on exacerbations of respiratory symptoms and on pulmonary function in patients with cystic fibrosis. N Engl J Med. 1994; 331 :637–642. [PubMed: 7503821]
46. Liew CW, Bochenski J, Kawamori D, Hu J, Leech CA, Wanic K, Malecki M, Warram JH, Qi L, Krolewski AS, Kulkarni RN. The pseudokinase tribbles homolog 3 interacts with atf4 to negatively regulate insulin exocytosis in human and mouse beta cells. J Clin Invest. 2010; 120 :2876–2888. [PubMed: 20592469]
47. Karlas T, Weise L, Kuhn S, Krenzien F, Mehdorn M, Petroff D, Linder N, Schaudinn A, Busse H, Keim V, Pratschke J, et al. Correlation of cell-free DNA plasma concentration with severity of non-alcoholic fatty liver disease. J Transl Med. 2017; 15 :106. [PubMed: 28521774]
48. Dicker AJ, Crichton ML, Pumphrey EG, Cassidy AJ, Suarez-Cuartin G, Sibila O, Furrie E, Fong CJ, Ibrahim W, Brady G, Einarsson GG, et al. Neutrophil extracellular traps are associated with disease severity and microbiota diversity in patients with chronic obstructive pulmonary disease. J Allergy Clin Immunol. 2018; 141 :117–127. [PubMed: 28506850]

Europe PMC Funders Author Manuscripts

Highlights

- NETs elicit a systemic DNase response in a feedback mechanism which is critical for clearance of NETs and inflammation resolution.
- Hypercholesterolemia in *Apoe*$^{-/-}$ mice leads to defective NET-induced DNase response and aberrant persistence of NETs and exacerbated inflammation.
- NET-induced DNase response is impaired via an ER stress dependent mechanism during hypercholesterolemia.
- Correction of defective DNase response by exogenous supplementation of DNase1 leads to lower lesional inflammation and beneficial plaque remodeling in an *Apoe*$^{-/-}$ mouse model of advanced atherosclerosis.

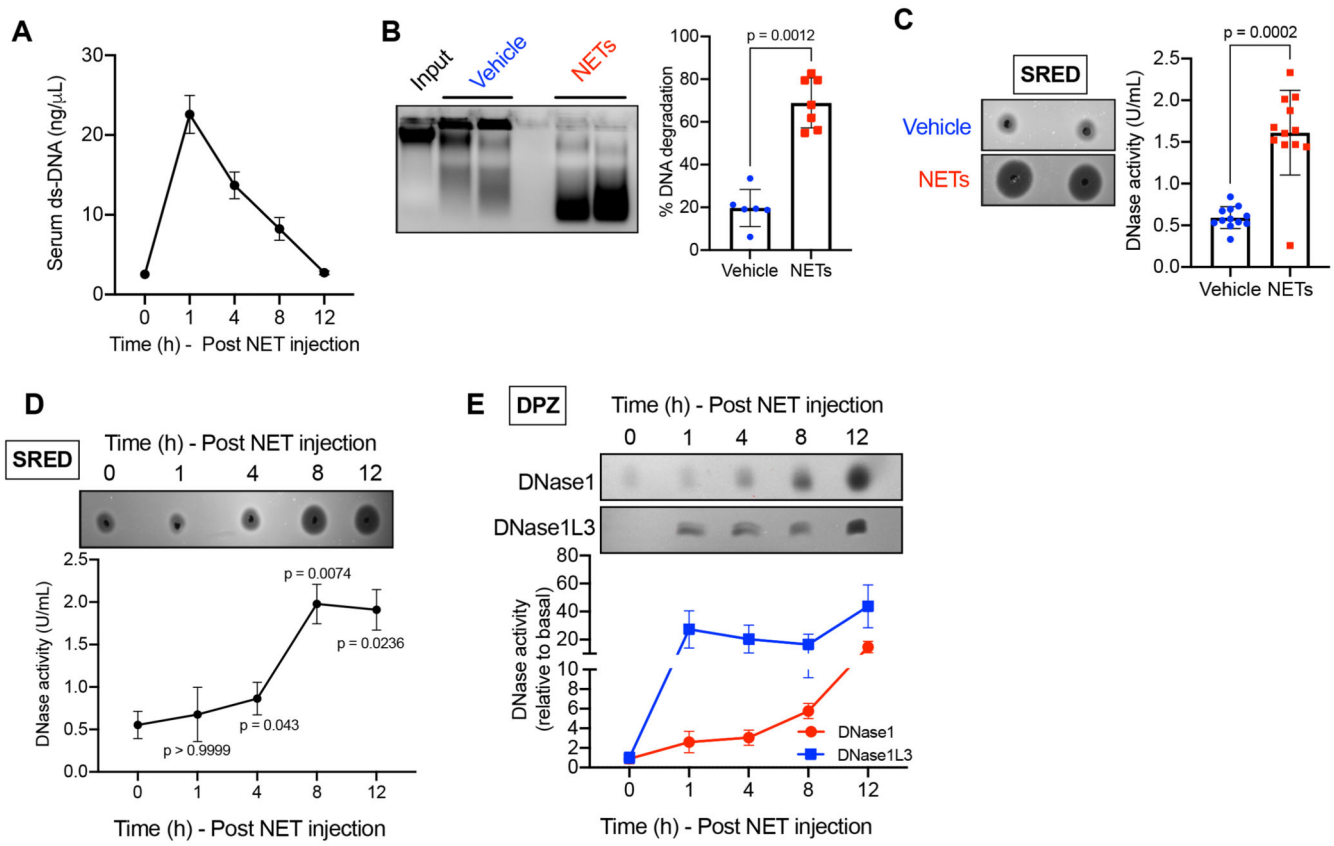

Figure 1. Increase in extracellular NETs elicits a systemic DNase response.

Female C57BL/6J mice were administered NETs (40 μg) intravenously followed by collection of blood at periodic intervals as indicated. (**A**) Sera of mice were analyzed for the levels of extracellular ds-DNA using Qubit fluorometric assay. (**B**) Sera collected at 12 h from vehicle or NET-injected mice were incubated with input DNA for 2.5 h followed by agarose gel electrophoresis. The scatter plot on the right represents quantified data of the extent of DNA degradation expressed as a percentage of the input DNA (n= 6 mice in vehicle-treated and 7 mice in NET-treated group). (**C**) Single radial enzyme diffusion (SRED) assay to quantify total DNase activity in the serum collected at 12 h from vehicle or NET-injected mice. The scatter plot represents the quantified data of DNase activity in the two groups of mice obtained by interpolation from known DNase standards. n = 12 female mice in each group. (**D**) Similar to (C) except that SRED was conducted on sera collected from NET-injected mice at indicated time points. (**E**) Depolymerizing polyacrylamide gel electrophoresis zymography (DPZ) assay to analyze expression levels of DNase1 and DNase1L3 in the sera of NET-injected mice at the indicated time points. n = 4 female mice per group. Tests for normality and equal variance were conducted using Shapiro-Wilk test and Brown-Forsythe test respectively. p values were determined by Mann-Whitney test (**B and C**) or Kruskal-Wallis and Dunn's multiple comparisons test (**D**).

Europe PMC Funders Author Manuscripts

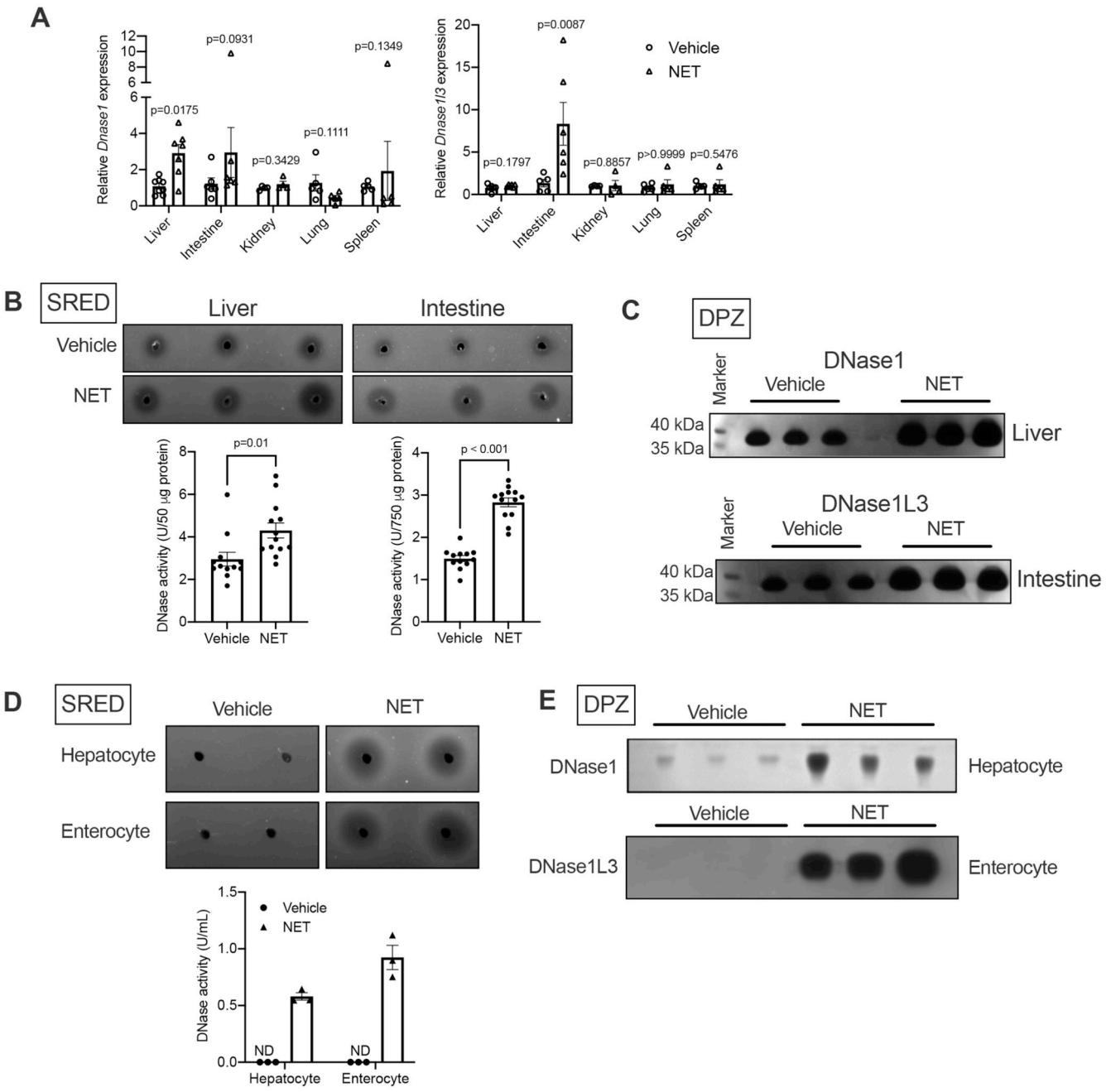

Figure 2. Liver and intestine respond to systemic increase in NET levels and secrete DNase1 and DNase1L3 respectively.

(**A**) qPCR-based analysis of gene expression of DNase1 and DNase1L3 in indicated organs of mice injected either vehicle or NET. n = 5 mice per group. (**B**) SRED assay to measure total DNase activity in liver and intestine of vehicle or NET injected mice. (**C**) DPZ for quantification of DNase1 levels in lysates of liver (top panel) and intestine (bottom panel) of mice injected with either vehicle or NET. (**D and E**) HepG2 cells (Hepatocytes) or Caco2 cells (Enterocytes) were incubated without or with NET and the cell culture supernatants were assayed for total DNase activity by SRED (D) or DNase1 and DNase1L3 activity by

DPZ (E). The data from 3 independent biological replicates are presented. Data in (A) and (B) were analyzed for normality using Shapiro-Wilk test and p values were calculated using Mann-Whitney test (**A**) or Student's 2-tailed t-test (**B**).

Europe PMC Funders Author Manuscripts

Europe PMC Funders Author Manuscripts

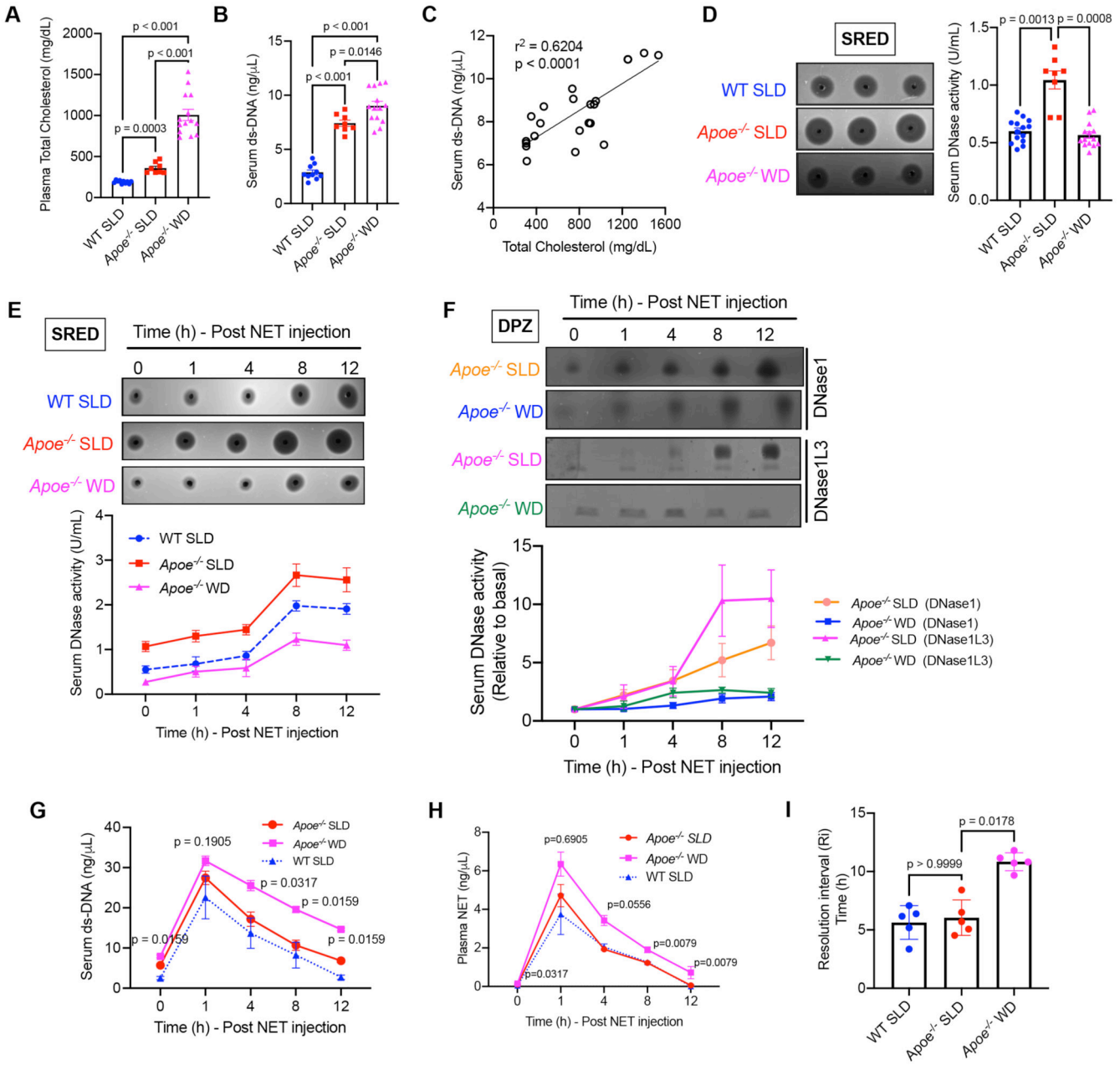

Figure 3. Hypercholesterolemia impairs the NET-induced DNase response.

8 wk-old male C57BL/6J mice and *Apoe*$^{-/-}$ mice were fed either a standard laboratory diet (SLD) or a western-type diet (WD) for 3 wks as indicated. (**A**) Measurement of plasma total cholesterol in indicated groups of mice. n = 8-14 mice per group. (**B**) The serum extracellular ds-DNA levels were measured in the indicated groups of mice using the Qubit fluorescence assay (n = 8-14 mice group). (**C**) The plot represents correlation between total cholesterol levels and serum extracellular ds-DNA concentration in standard laboratory diet and WD fed *Apoe*$^{-/-}$ mice. Linear regression was conducted to analyze correlation between the two parameters. (**D**) Quantification of basal total serum DNase activity by SRED in WT and *Apoe*$^{-/-}$ mice after 3 wks on indicated diet. (**E-H**) The three groups of mice were

administered NETs intravenously and sera was isolated at periodic intervals as indicated and subjected to analysis of (**E**) total serum DNase activity by SRED, (**F**) analysis of DNase1 and DNase1L3 activity by DPZ, (**G**) analysis of extracellular DNA levels, (**H**) analysis of plasma NET levels, and (**I**) analysis of resolution interval defined as the time taken for the extracellular DNA levels to reach half-maximal. n = 5 mice per group. All data sets were analyzed for normality using Shapiro-Wilk test. p values were obtained using Brown-Forsythe and Welch ANOVA with Dunnett's multiple comparisons test (**A, B, and D**), Kruskal-Wallis and Dunn's multiple comparison test (**I**), or Mann-Whitney test (**G and H**).

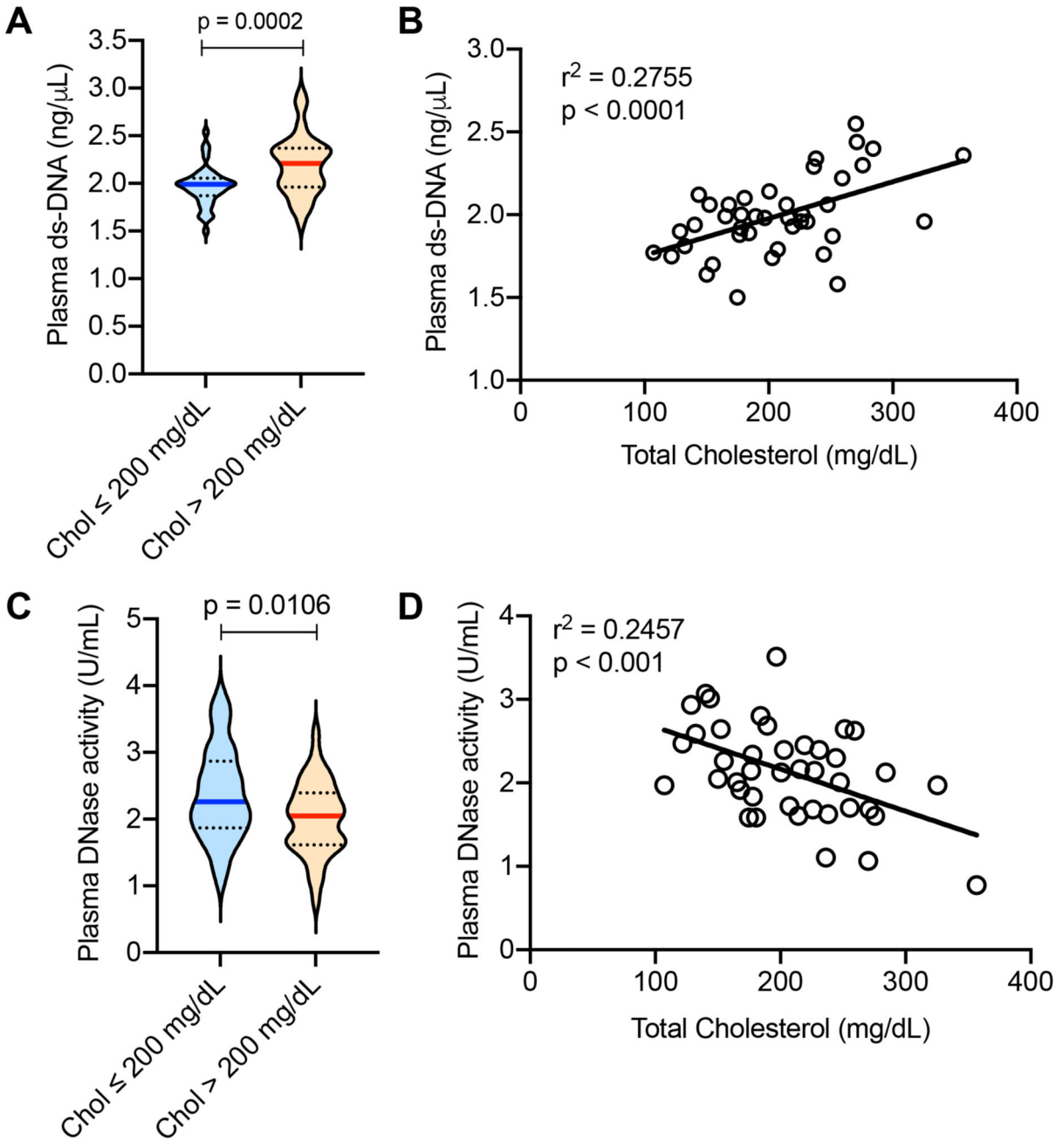

Figure 4. Hypercholesterolemia is associated with increased extracellular DNA and decreased plasma DNase activity in humans.

Plasma was isolated from healthy adults of both sexes. (**A and C**) Analysis of plasma extracellular ds-DNA levels by Qubit fluorometric assay and total DNase activity by SRED respectively in individuals with total plasma cholesterol levels < 200 mg/dL (normocholesterolemia) or > 200 mg/dL (hypercholesterolemia). n = 41 per group. (**B and D**) Analysis of correlation between total plasma cholesterol concentration with extracellular ds-DNA levels or total DNase activity respectively. n = 41. Data sets were analyzed by

Shapiro-Wilk test for normality. p values were obtained by parametric 2-tailed t-test (**A and C**). Simple linear regression was conducted to analyze correlation (**B and D**).

Europe PMC Funders Author Manuscripts

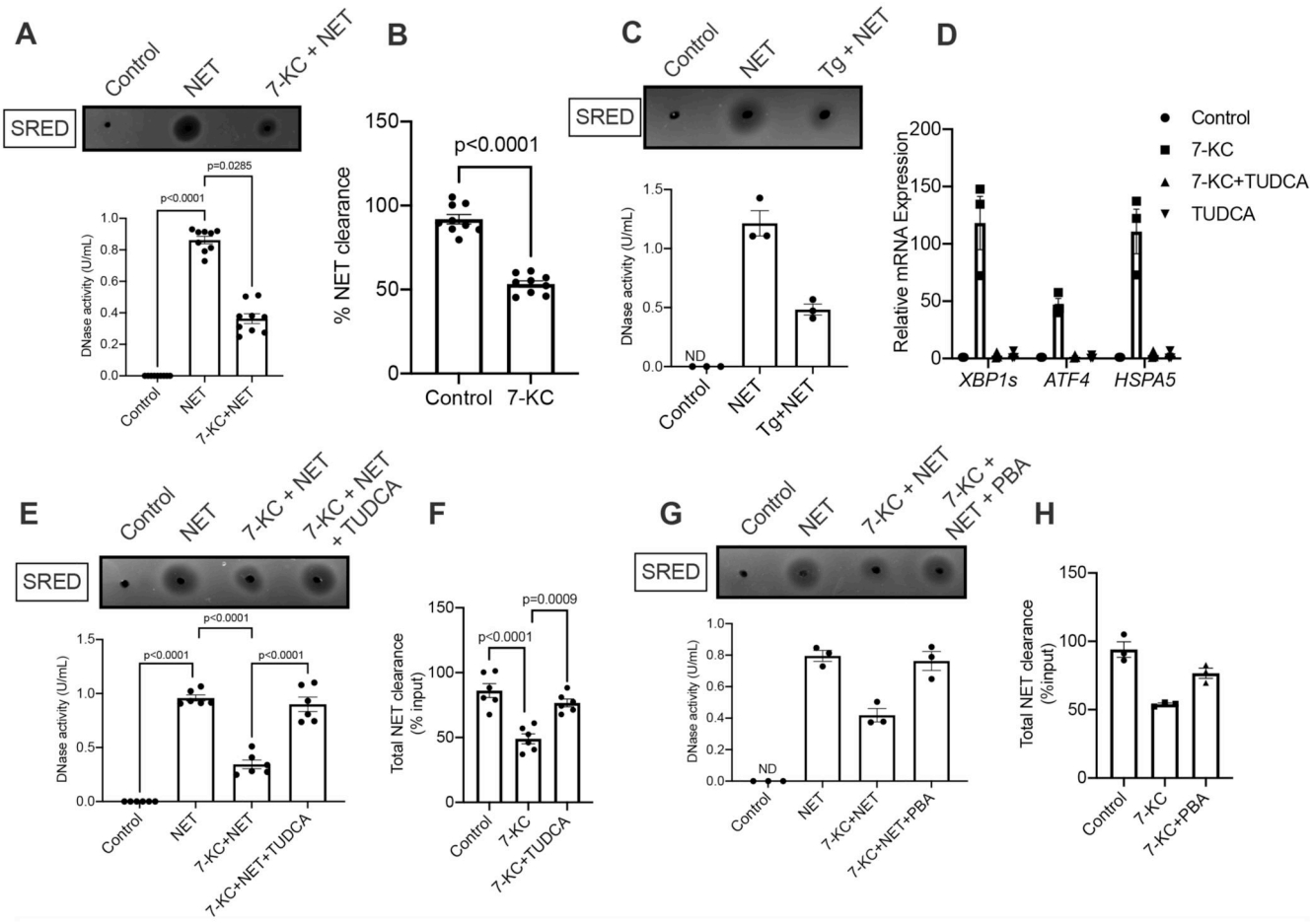

Figure 5. Lipid-induced ER stress impairs the NET-induced DNase response *in vitro*.

(**A**) Quantification of total DNase activity in the culture supernatants of control HepG2 cells or 7-KC treated HepG2 cells incubated with NETs for 12 h. (**B**) The amount of remaining extracellular ds-DNA in the cell culture supernatants of control or 7-KC-treated HepG2 cells incubated with 10 μg NETs for 12 h was analyzed by Qubit assay. The graph represents the efficiency of NET clearance as a percentage of input NETs. The data presented in panels (A) and (B) are plotted from 9 biological replicates pooled from 3 independent experiments. (**C**) Quantification of total DNase activity in cell culture supernatants of HepG2 cells treated without or with thapsigargin (Tg) and incubated with NETs for 12 h. (**D**) Analysis of expression levels of ER stress related genes by qPCR in appropriate group of HepG2 cells as indicated. n = 3 biological replicates. (**E**) Measurement of NET-induced DNase response in culture supernatants of HepG2 cells treated with 7-KC in the absence or presence of TUDCA. (**F**) Quantification of efficiency of NET clearance from the supernatant of HepG2 cells treated with 7-KC in the absence or presence of TUDCA. The data presented in panels (E) and (F) are plotted from 6 biological replicates pooled from 2 independent experiments. (**G and H**) Similar to E and F, except that HepG2 cells were treated with PBA instead of TUDCA. The data are presented as Mean±SEM from 3 independent biological replicates. ND, not detected.

Europe PMC Funders Author Manuscripts

Europe PMC Funders Author Manuscripts

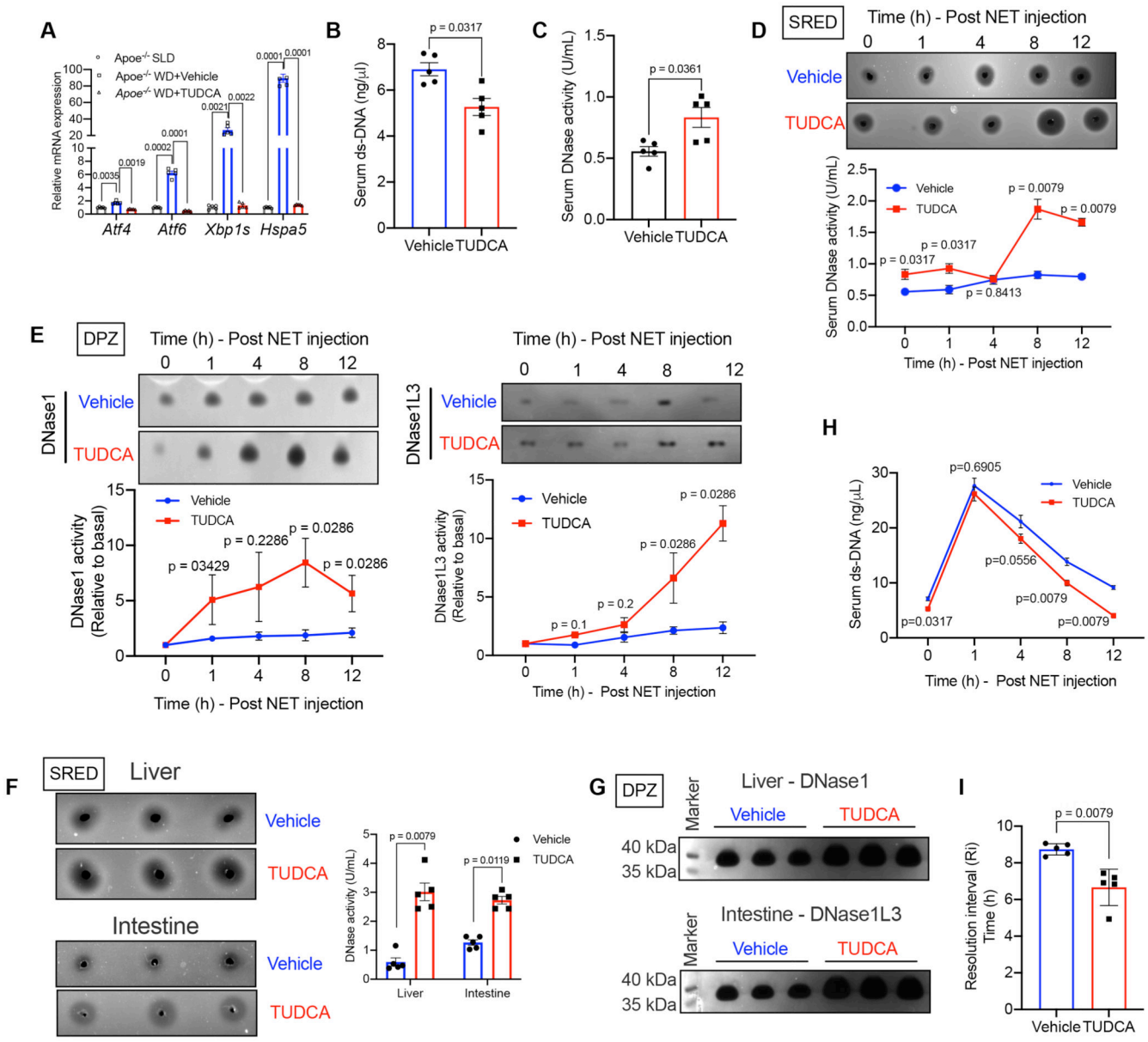

Figure 6. TUDCA rescues the defective NET-induced DNase response in hypercholesterolemic *Apoe*$^{-/-}$ mice.

10-wk old female *Apoe*$^{-/-}$ mice were fed WD for 3 wks with concomitant daily administration of either vehicle or TUDCA intraperitoneally. (A) qPCR-based analysis of expression levels of ER stress responsive genes Atf4, Atf6, Xbp1s, and Hspa5 in the liver of indicated groups of mice. (B) Analysis of basal serum extracellular ds-DNA levels and (C) total DNase activity in vehicle and TUDCA-treated mice. (D) SRED-based quantification of total DNase activity, (E) DPZ-based analysis of DNase1 and DNase1L3 expression levels. (F) Quantification of total DNase activity by SRED assay in liver and intestine of NET-injected WD-fed *Apoe*$^{-/-}$ mice treated with vehicle or TUDCA. (G) Analysis of relative expression levels of DNase1 in the liver and DNase1L3 in the intestine of NET-injected WD-fed *Apoe*$^{-/-}$ mice treated with vehicle or TUDCA. (H) Measurement of serum

extracellular ds-DNA levels at indicated time points post-injection of NET in vehicle and TUDCA-treated mice. (I) Quantification of resolution interval, which is the time in hours for the extracellular ds-DNA levels to reach half-maximal in vehicle and TUDCA-treated mice. n = 5 mice per group. Mann-Whitney test was conducted to analyze statistical significance (**A-I**).

Europe PMC Funders Author Manuscripts

Europe PMC Funders Author Manuscripts

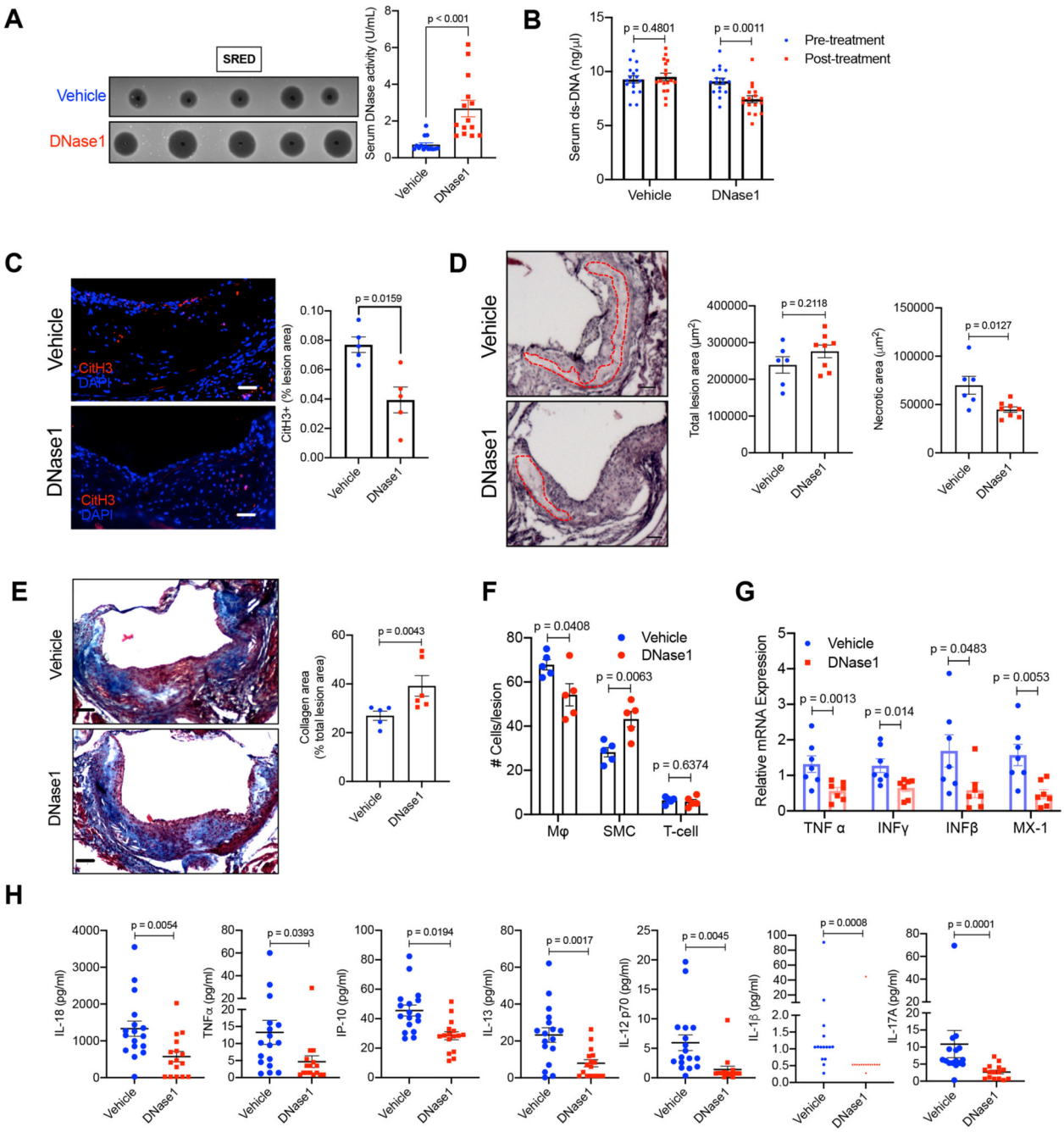

Figure 7. Exogenous DNase1 administration promotes atherosclerotic plaque remodeling and stabilization.

Female *Apoe*$^{-/-}$ mice were fed western-type diet for 16 wks followed by administration of either vehicle or DNase1 (400 U) intravenously 3 times a week for 4 weeks. (**A**) SRED analysis of serum total DNase activity in vehicle or DNase1-injected mice. (**B**) Analysis of serum extracellular ds-DNA concentration in indicated groups of mice before and after treatment with vehicle or DNase1. (**C**) Aortic root sections of vehicle and DNase1-treated mice were immunostained with antibody against CitH3 (red) and percent lesion area that

stains positive for CitH3 was quantified. Nucleus were stained with DAPI (blue). Bar, 25 μm. n = 5 mice per group. (**D**) H&E staining of aortic root sections of vehicle and DNase1-treated mice to quantify the total lesion area and the total necrotic area (red dotted line). Bar, 25 μm. (**E**) Mason trichrome staining of aortic root sections of vehicle and DNase1-treated mice to quantify collagen deposition in the plaque. Bar, 25 μm. (**F**) Immunofluorescence-based quantification of percent macrophages (F4/80), smooth muscle cells (sm-Actin), and T-cells (CD3) in atherosclerotic lesions of vehicle and DNase1-treated mice. (**G**) qPCR-based analysis of relative mRNA expression of indicated pro-inflammatory genes in aorta of vehicle and DNase1-treated mice. (**H**) Multiplex ELISA for quantification of pro-inflammatory cytokine levels in the sera of vehicle and DNase1-treated mice. Shapiro-Wilk test was conducted to determine normality of data sets. p values were calculated using Mann-Whitney test (**A, C, and E**), Wilcoxon paired test (**B**), or Student's t-test (**D, F-H**).

Europe PMC Funders Author Manuscripts

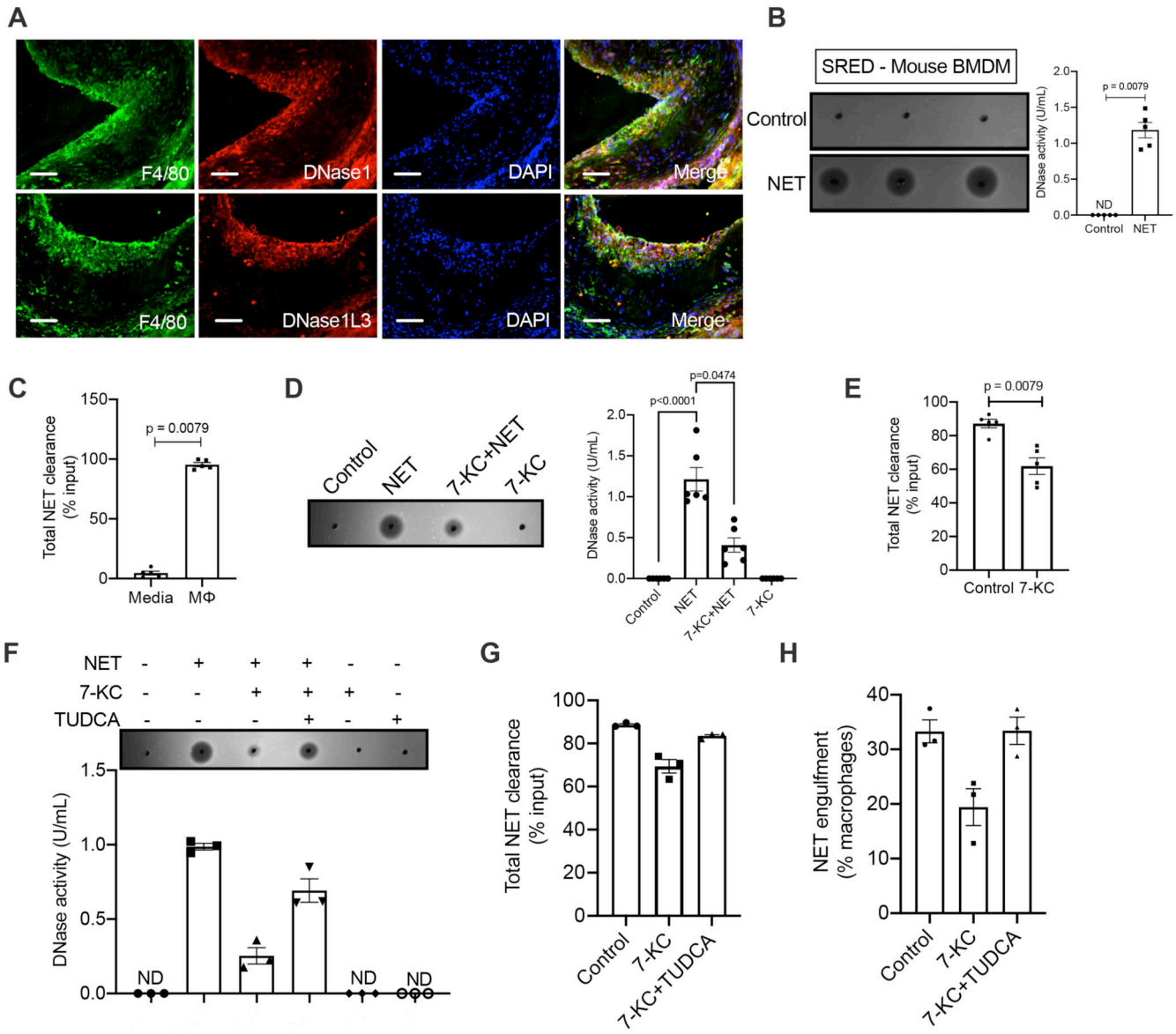

Figure 8. Macrophages secrete DNases in response to NETs.

(**A**) Aortic root sections of 16 wk WD-fed female *Apoe*$^{-/-}$ mice were immunostained with anti-DNase1 antibody (top panel) or anti-DNase1L3 antibody (bottom panel) and their expression colocalized with macrophages stained with anti-F4/80 antibody (green). Nucleus was counterstained with DAPI (blue). Bar, 50 μm. (**B**) SRED assay for quantification of total DNase activity in the culture supernatants of murine BMDM either left untreated or treated with NETs (10 μg) for 12 h.(**C**) Qubit fluorometric analysis of remaining input DNA after 12 h incubation with either cell culture media or macrophages. The data are represented as percent of input DNA that has been cleared from the media or supernatant. (**D**) SRED for quantification of total DNase activity in the cell culture supernatants of the indicated group of BMDMs. n = 6 biological replicates pooled from 2 independent experiments. (**E**) Qubit fluorometric analysis of the total NET clearance efficiency. (**F**)

SRED-based analysis of total DNase activity in cell culture supernatants of indicated groups of macrophages. (**G**) Qubit fluorometric analysis of the total NET clearance efficiency and (**H**) NET engulfment efficiency of indicated group of macrophages. p values were determined using Mann-Whitney test (**B, C, and E**). Data in panels F, G, and H are presented as Mean±SEM from 3 independent biological replicates. ND, not detected.

Europe PMC Funders Author Manuscripts